



OPEN

## Optimization of glutaraldehyde concentration in relation to swelling behavior of PVA-PEG-BTB film using hybrid genetic metaheuristic algorithm

Daeuk Kim<sup>1,2</sup>✉, Izabelle Nisha Maxine D. Chan<sup>1,2</sup>, Tossa Mae S. Manalastas<sup>2,3</sup>,  
Ronnie S. Concepcion II<sup>1,2</sup>, Joseph Rey H. Sta. Agueda<sup>1,2</sup> & Rafael Kyle B. Bitangcor<sup>4</sup>

The crosslinking characteristics of hydrogels and polymeric films critically influence their swelling capacity, a key factor in wound care applications. This study optimized the swelling behavior of polyvinyl alcohol (PVA)–polyethylene glycol (PEG)–bromothymol blue (BTB) films using three hybrid metaheuristic algorithms: Hybrid Genetic-Hippopotamus Optimizer (HG-HO), Hybrid Genetic-Walrus Optimization Algorithm (HG-WOA), and Hybrid Genetic-Horned Lizard Optimization Algorithm (HG-HLOA). Among these, HG-HLOA achieved the fastest convergence, while all algorithms reliably identified optimal solutions with comparable fitness values. The optimal glutaraldehyde concentration was determined as 4.9251 wt%, with a predicted maximum swelling ratio of 1217.7311%. Experimental validation yielded an average swelling ratio of 1225.7123%, differing by only 0.65% from the predicted value. An increasing trend in swelling ratio was observed with rising glutaraldehyde concentration up to the optimum point, followed by a decrease due to possible over-crosslinking and formation of acetal linkages. This trend was supported by structural analysis using Fourier Transform Infrared (FTIR) spectroscopy and Scanning Electron Microscopy (SEM). Statistical analysis via Analysis of Variance (ANOVA) confirmed a significant relationship between glutaraldehyde concentration and swelling ratio, with a p-value of  $2.1e^{-161}$ .

Glutaraldehyde (GA) is widely employed as a crosslinking agent across numerous biomedical applications, owing to its capacity to enhance the structural integrity and stability of polymers<sup>1</sup>. Crosslinked polymers exhibit improved mechanical properties, controlled degradation rates, and refined swelling behavior, making them highly suitable for applications requiring regulated absorption or release mechanisms. Such uses include hydrogels, wound care materials, tissue scaffolds, and drug delivery systems<sup>2</sup>. The integration of GA as a crosslinker in hydrogels and polymer films, for instance, has been shown to bolster material resilience and functionality significantly in these contexts<sup>1</sup>.

Swelling, defined as a material's capacity to retain fluid within its structural network, is a key parameter in assessing its responsiveness and suitability in diverse environments. The rate and extent of swelling are critical in predicting how materials behave when exposed to different immersion conditions, providing insight into the material's adaptability and functionality<sup>3</sup>. Hydrogels and crosslinked polymers are advantageous for wound care applications due to their moisture-retention capabilities. Among them, polyvinyl alcohol (PVA)-based hydrogels have been widely studied and valued for their superior swelling capacity, which is instrumental in fluid absorption and retention, making them viable candidates for wound management applications<sup>4,5</sup>.

The swelling properties of these materials are influenced by various factors, with crosslink density playing a particularly significant role. Swelling capacity is determined during hydration, as the material's hydrophilic polar groups interact with surrounding fluids. This interaction is governed by the material's surface porosity and the intermolecular spacing within its polymeric network. Crosslinker concentration is a critical factor influencing

<sup>1</sup>Department of Manufacturing Engineering and Management, De La Salle University, Manila 1004, Philippines.  
<sup>2</sup>Center of Engineering and Sustainable Development Research, De La Salle University, Manila 1004, Philippines. <sup>3</sup>Department of Chemical Engineering, De La Salle University, Manila 1004, Philippines. <sup>4</sup>Philippine Nuclear Research Institute, Department of Science and Technology, Quezon City 1101, Philippines. ✉email: daeuk\_kim@dlsu.edu.ph

these structural attributes, as it modulates the polymer network's density, ultimately impacting swelling behavior. Thus, controlling crosslink density through crosslinker concentration adjustments enables the fine-tuning of material performance in terms of fluid retention and response to hydration<sup>6,7</sup>.

The optimization of crosslinking parameters is essential to tailor the swelling behavior of polymers and hydrogels for specific applications. Conventionally, optimization in this field has been carried out using experimental design techniques like factorial design and response surface methodology (RSM). Factorial experimental design analyzes multiple factors by varying them simultaneously, allowing comprehensive exploration of all possible combinations, while RSM combines experimental design with optimization and regression analysis to model and optimize the relationship between independent factors and a response variable<sup>8</sup>. While conventional methods have been extensively used to optimize the ionic conductivity of polymeric membranes or adjust reaction conditions and material parameters<sup>9,10</sup>, they can become impractical in high-dimensional problems. These approaches often require numerous trials to capture complex interactions accurately and may struggle to handle non-linear or non-convex objective functions, limiting their effectiveness in more intricate optimization tasks.

Artificial intelligence (AI) has become a game-changing tool in scientific research and engineering, providing innovative approaches to optimization and decision-making. AI algorithms, particularly those in machine learning and optimization, enable researchers to analyze complex data, identify patterns, and predict outcomes more effectively than traditional approaches<sup>11,12</sup>. In particular, metaheuristic algorithms—flexible and powerful AI-based approaches—provide a significant advantage for high-dimensional, complex optimization challenges. Unlike traditional calculation methods, metaheuristics explore multiple stochastic pathways to identify optimal solutions, making them especially valuable when non-linear relationships between variables exist. Metaheuristic processes are derived from heuristic algorithms, which are methods that highly depend on the problem and only result in a local optimum solution. Thus, the innovation of such heuristic processes is featured in the metaheuristic algorithm, which investigates the search or solution space in a more thorough manner until convergence is made possible for the attainment of a desired optimal solution<sup>13</sup>.

Metaheuristic algorithms are commonly classified based on their behavioral characteristics, falling into four primary categories: physics-based, swarm-based, evolution-based, and human behavior-based algorithms<sup>14</sup>. Among these, swarm-based algorithms have garnered significant attention due to several core attributes that make them particularly robust and effective for optimization. They are straightforward to implement; each agent follows simple behavioral rules, making the system easy to develop and adjust. These algorithms also demonstrate strong scalability, as each individual's limited perceptual reach allows the system to adapt seamlessly to varying group sizes without compromising performance. A further advantage is their intrinsic capacity for autonomous coordination, where complex group behaviors emerge naturally from interactions between individuals without a central controller. Lastly, swarm-based algorithms exhibit inherent concurrency and decentralized processing, with the collective actions of individuals lending themselves to simultaneous operations, making them highly suitable for computationally intensive tasks<sup>15</sup>.

Popular swarm-based algorithms, including Ant Colony Optimization (ACO), Grey Wolf Optimizer (GWO), Particle Swarm Optimization (PSO), and Artificial Bee Colony (ABC), have proven effective across a range of optimization problems. However, their application in polymer optimization remains relatively underexplored, with previous studies primarily utilizing RSM for such purposes. Recent advancements in optimization algorithms have increasingly drawn inspiration from animal behaviors, particularly hunting and foraging strategies. Algorithms such as the Fossa Optimization Algorithm (FOA), Orangutan Optimization Algorithm (OOA), and Spider-Tailed Horned Viper Optimization (STHVO) exemplify this trend by mimicking the behavioral patterns of their biological counterparts. These nature-inspired approaches typically adopt population-based frameworks, wherein a group of candidate solutions cooperatively navigates and optimizes the search space to find optimal or near-optimal solutions<sup>16-18</sup>. This study applies such advanced swarm-based metaheuristic algorithms, integrated with genetic programming, to optimize glutaraldehyde concentration concerning the swelling behavior of a hydrogel film.

To achieve this, bio-inspired optimizers such as the Hippopotamus Optimizer (HO), Walrus Optimization Algorithm (WOA), and Horned Lizard Optimization Algorithm (HLOA) were selected for their innovative search mechanisms and shared network architecture, which enhances their effectiveness. These algorithms mimic the adaptive strategies of their respective species, leveraging cooperative and exploratory behaviors to navigate complex optimization landscapes. The HO models territorial and social dynamics, effectively balancing exploration of the search space and refinement toward optimal solutions<sup>19</sup>. The WOA mimics the dual-phase behaviors of walrus groups, alternating between broad exploration during foraging and focused exploitation during resting phases<sup>20</sup>. The HLOA dynamically adjusts its search patterns based on survival strategies like camouflage and escape, allowing it to efficiently navigate rugged and dynamic solution spaces<sup>21</sup>. This population-based approach, combined with adaptive mechanisms, allows these algorithms to efficiently handle complex optimization challenges while avoiding local optima.

Traditional optimization techniques, such as Response Surface Methodology (RSM), have been widely used in polymer research to model and optimize material properties. However, RSM often assumes a predefined functional relationship between variables, which may not fully capture the nonlinear and intricate interactions that govern polymer behavior, particularly in hydrogels designed for biomedical applications. To address this limitation, this study integrates advanced bio-inspired metaheuristic algorithms to optimize the swelling capacity of halochromic hydrogel films for chronic wound care applications. By utilizing the adaptive and exploratory capabilities of these algorithms, the proposed approach offers a more robust and flexible optimization framework. This ensures enhanced hydrogel performance and functionality.

The key contributions of this study are:

- Exploration of the applicability of bio-inspired hybrid genetic optimization algorithms in material science, showcasing their potential for addressing complex polymer optimization challenges;
- Development of advanced hydrogel films with tailored swelling properties, enhancing their application in chronic wound care and other biomedical uses;
- Demonstration of the scalability of the optimization approach, highlighting its potential for broader applications in biotechnology, healthcare, and advanced materials research; and
- Provision of multidisciplinary insights of effect of glutaraldehyde concentration in relation to swelling behavior by integrating gel fraction tests, FTIR, and SEM, offering a comprehensive characterization of the material's behavior.

The succeeding sections of this paper are structured as follows: Results present the outcomes of the optimization process and experimental validation of the hydrogel's swelling behavior. Discussion provides an in-depth analysis of the findings, explaining the influence of glutaraldehyde concentration on hydrogel properties and the effectiveness of the proposed optimization algorithms. Conclusion summarizes the key insights, highlights the study's contributions, and suggests directions for future research. Finally, Methods detail the experimental procedures, optimization framework, and characterization techniques used to evaluate the hydrogel formulation.

## Results

### Swelling ratio of PVA-PEG-BTB film

The swelling behavior of polyvinyl alcohol (PVA)–polyethylene glycol (PEG)–bromothymol blue (BTB) films was analyzed as a function of glutaraldehyde (GA) concentration, with detailed results illustrated in Figs. 1 and 2. Swelling kinetics analysis revealed a rapid water uptake phase during the first 30 min, followed by a plateau after approximately 60 min, with films crosslinked at 5.0 wt% GA achieving the highest equilibrium swelling ratio (~ 1200%) as shown in Fig. 1. In comparison, films with lower GA concentrations (0.5–2.0 wt%) exhibited moderate swelling capacities, stabilizing below 900%. Conversely, films with higher GA concentrations (> 5.0 wt%) displayed reduced swelling ratios and slower kinetics, suggesting that overly dense crosslinking impedes water diffusion and retention. Figure 2 demonstrates the maximum swelling ratio and variability of each PVA-PEG-BTB film with different glutaraldehyde concentrations. The maximum swelling ratio exhibited a distinct trend, increasing with GA concentration and peaking at approximately 1200% for films crosslinked with 5.0 wt% GA. Beyond this concentration, a decline in the swelling ratio was observed, likely due to excessive crosslinking reducing the availability of hydrophilic sites for water absorption. Variability in swelling performance was also evident across the GA concentration range. Films in the 5.0–5.5 wt% GA range not only exhibited the highest swelling ratios but also demonstrated greater variability, potentially reflecting the balance between crosslink density and structural integrity at these concentrations. In contrast, films with both lower and higher GA concentrations exhibited narrower distributions and lower swelling capacities, indicating more uniform but less effective swelling behavior.

### Optimization using hybrid genetic metaheuristic algorithms

To determine the fitness function describing the relationship between glutaraldehyde (GA) concentration and the maximum swelling ratio, genetic programming was utilized. The resulting fitness function is expressed as:

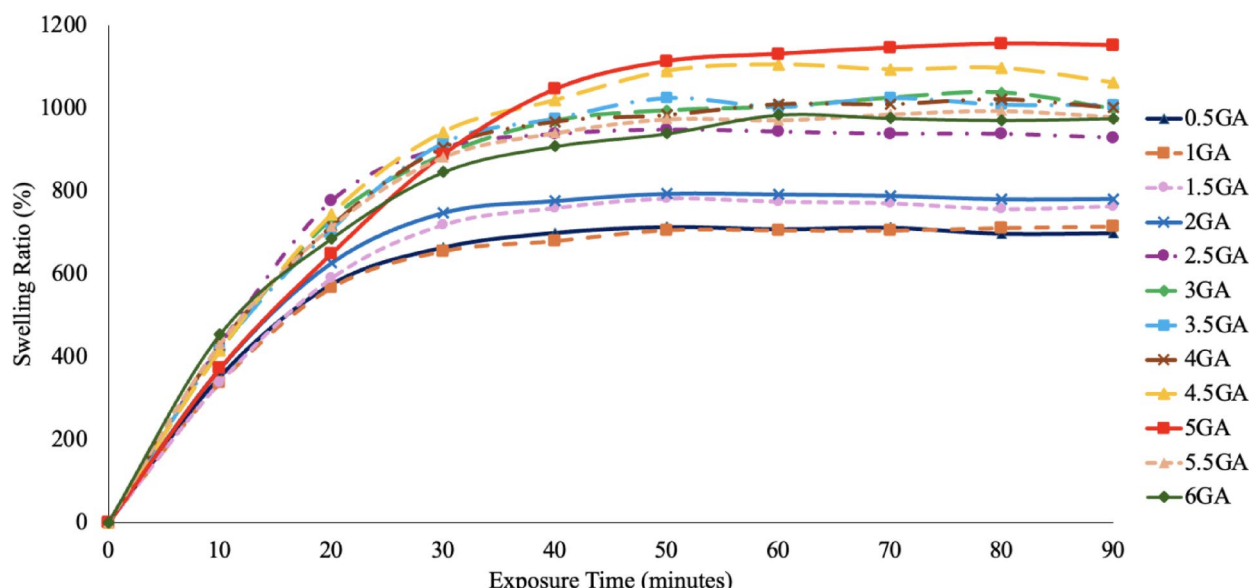


**Fig. 1.** Swelling behavior of PVA-PEG-BTB film with varying glutaraldehyde concentrations over 90 min.

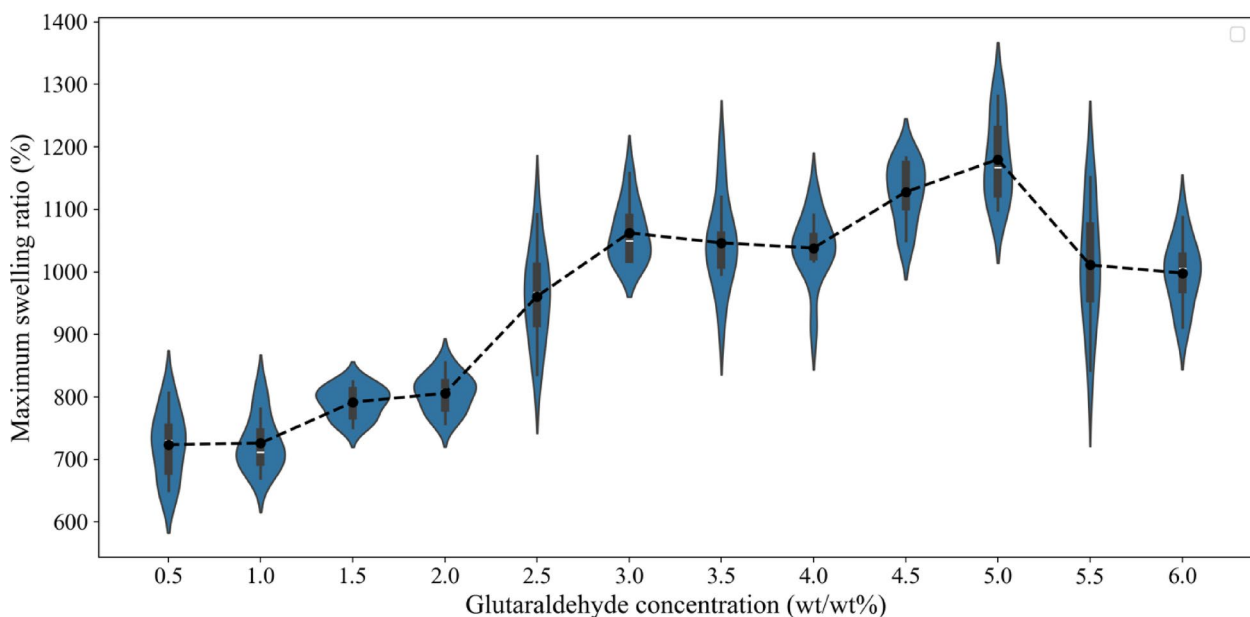


**Fig. 2.** Maximum swelling ratio of each PVA-PEG-BTB film.

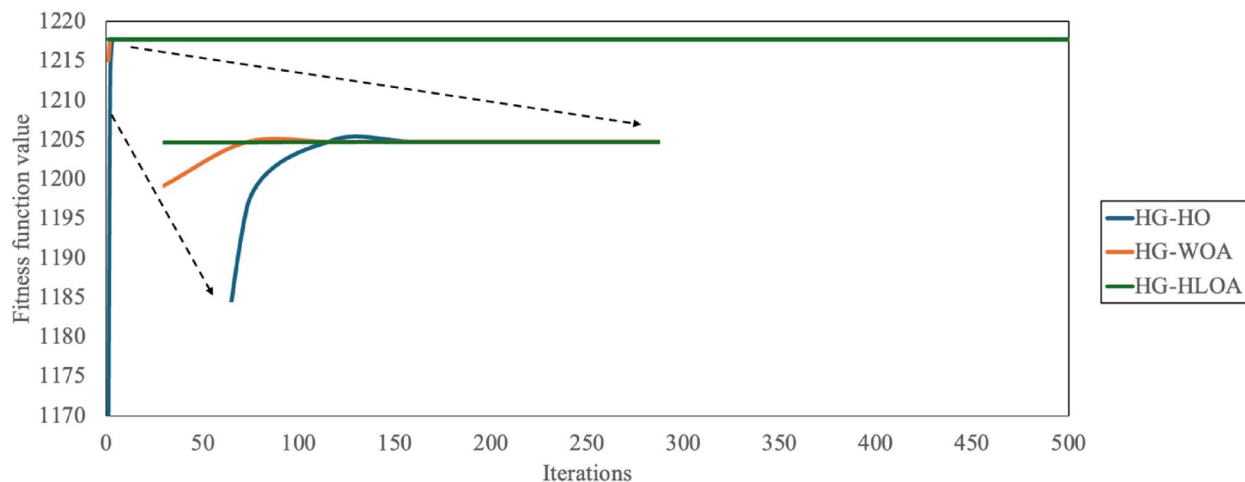


**Fig. 3.** Convergence curves of the three metaheuristic algorithms namely, HG-HO, HG-WOA and HG-HLOA, in optimizing the glutaraldehyde concentration in relation to swelling behavior of PVA-PEG-BTB film.

$$f(x) = 974 - 146\sin\left(\sin\left(x^{\frac{3}{2}}\right)\right) - 146\sin(\sin(x)) \quad (1)$$

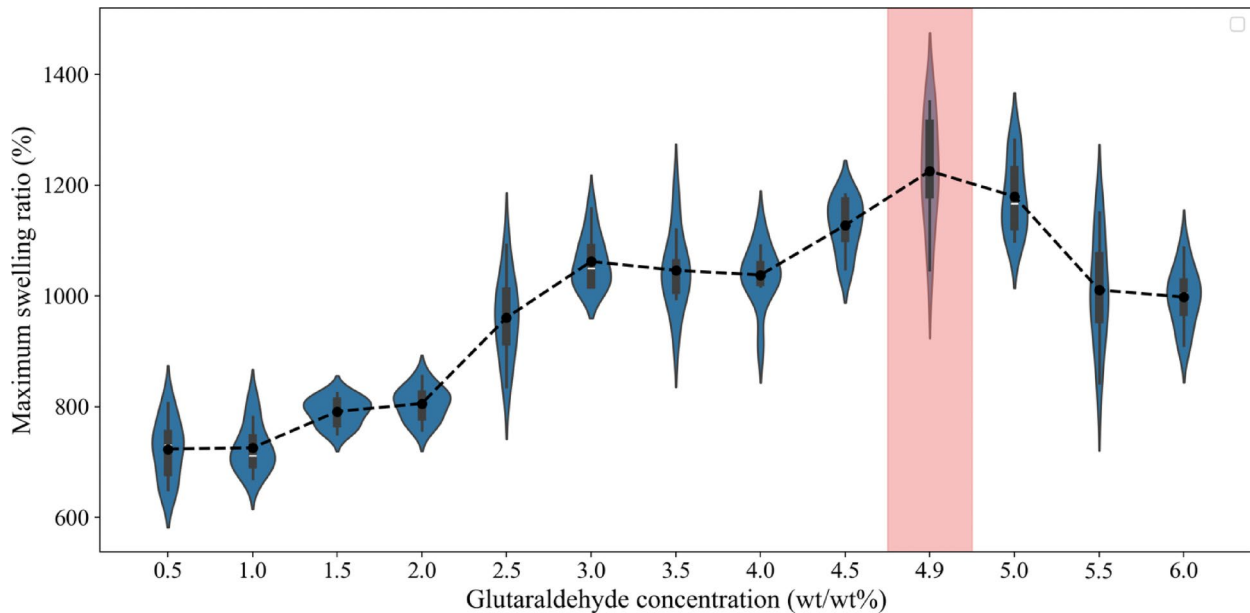
where  $f(x)$  represents the fitness value, corresponding to the maximum swelling ratio, and  $x$  denotes the GA concentration. The equation above combines a baseline constant (bias) with two nonlinear transformations of the input  $x$ . The bias term, 974, serves as the starting value for the output, representing the model's base prediction before any adjustments are made. The first transformation involves raising  $x$  to the power of  $3/2$ , followed by applying two nested sine functions. The second transformation applies the same nested sine functions but directly to  $x$ . Both transformations are weighted equally with a coefficient of  $-146$ , indicating that they have identical magnitudes of influence on the model's output but work to reduce it due to their negative weights. This structure allows the model to capture complex, nonlinear relationships in the data while starting from a high base value and adjusting downward based on the nonlinear contributions of the two genes. The equal weighting of the genes suggests that they are equally important in the model's prediction, though their specific influence depends on the input  $x$ .

The convergence analysis of the three optimization algorithms—Hybrid Genetic-Hippopotamus Optimizer (HG-HO), Hybrid Genetic-Walrus Optimization Algorithm (HG-WOA), and Hybrid Genetic-Horned Lizard Optimization Algorithm (HG-HLOA)—revealed significant differences in their performance (Fig. 3). The HG-

Iteration	HG-HO	HG-WOA	HG-HLOA
1	1168.4319	1215.0359	1217.7311
2	1213.5254	1217.6993	1217.7311
3	1217.7302	1217.7290	1217.7311
4	1217.7302	1217.7290	1217.7311
5	1217.7302	1217.7311	1217.7311
6	1217.7304	1217.7311	1217.7311
7	1217.7311	1217.7311	1217.7311
8	1217.7311	1217.7311	1217.7311

**Table 1.** Fitness function value of each optimization algorithm from 1 st to 8 th iteration.

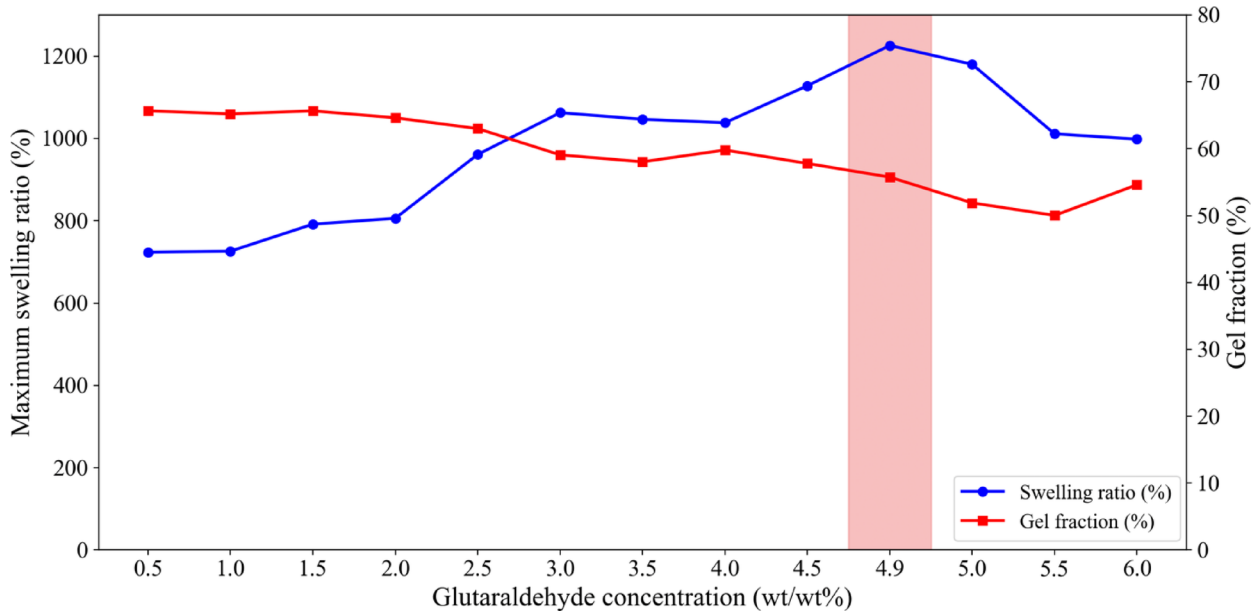
	HG-HO	HG-WOA	HG-HLOA
Best solution (Optimal GA concentration)	4.9251	4.9251	4.9251
Fitness value (Maximum swelling ratio)	1217.7311	1217.7311	1217.7311

**Table 2.** Best solution and fitness value of each optimization algorithm.**Fig. 4.** Maximum swelling ratio of each PVA-PEG-BTB film with optimized values highlighted.

HLOA algorithm exhibited the fastest convergence, reaching the optimal fitness function value of 1217.7311 in the first iteration and maintaining it throughout. This superior stability and efficiency make HG-HLOA the most effective approach. Table 1 presents the fitness values across the first eight iterations, highlighting the differences in convergence behavior.

Table 2 presents the optimal GA concentration identified by all three optimization algorithms, consistently determined as 4.9251 wt%, with a predicted maximum swelling ratio of 1217.7311%. Experimental validation yielded an average swelling ratio of 1225.7123%, differing by only 0.65% from the predicted value, demonstrating strong agreement between the model and experimental results. Figure 4 illustrates the swelling ratio trends across various GA concentrations, highlighting the optimized value. The consistency across optimization methods confirms the robustness and reliability of the proposed framework in predicting and optimizing polymeric film performance. Furthermore, Table 3 provides a comparative analysis with previous studies utilizing response surface methodology (RSM), emphasizing the superior predictive accuracy and optimization efficiency of the proposed hybrid genetic approach.

Optimization method	Input variable	Response parameter	Percent difference (%)	Reference
RSM	Rice starch & curcumin concentrations	Tensile strength	0.65	22
		Elongation at break	19.64	
		Water vapor permeability	42.72	
		Antioxidant properties	2.03	
RSM	Alginate ratio, crosslinking time, crosslinker concentration, culture media, UV exposure	Degradation time	5.62	23
		Swelling ratio	8.84	
Hybrid genetic metaheuristic algorithm	Glutaraldehyde concentration	Swelling ratio	0.65	This work

**Table 3.** Comparison of other related studies and this work.**Fig. 5.** Maximum swelling ratio and gel fraction per varying glutaraldehyde concentration with optimized values highlighted.

### PVA-PEG-BTB film characterization and analysis

#### Gel fraction vs. swelling behavior

The effects of glutaraldehyde concentration on the maximum swelling ratio (%) and gel fraction (%) of the polymeric films are presented in Fig. 5. The maximum swelling ratio exhibited an increasing trend with rising glutaraldehyde concentration, starting at approximately 600% for films with 0.5 wt/wt% glutaraldehyde and peaking at around 1200% at 4.9 wt/wt%. Beyond this concentration, the swelling ratio began to decline, dropping to approximately 1000% at 6 wt/wt% and continuing to decrease at higher concentrations of 7 wt/wt% and 10 wt/wt% (cf. supplementary figure S1). The initial increase in swelling ratio with rising glutaraldehyde concentration, though contrasting with typically reported studies<sup>24</sup>, can be attributed to the hydrophilic nature of glutaraldehyde.

In contrast, the gel fraction followed a different pattern, remaining relatively stable at approximately 65–70% up to 2.5 wt/wt% glutaraldehyde, then gradually declining to around 50% at higher concentrations. Interestingly, the gel fraction showed an anomalous increase at 6 wt/wt% glutaraldehyde, suggesting that further crosslinking occurred. This behavior is likely due to excessive crosslinking, which rigidifies the polymer network and reduces its ability to expand and absorb water<sup>25</sup>.

#### Fourier transform infrared spectroscopy (FTIR) and scanning electron microscopy (SEM) surface morphology analysis

For the FTIR and SEM analyses, the key concentrations identified from the gel fraction test—1 wt%, 2.5 wt%, 4.9 wt% (optimized concentration), and 5.5 wt%—were selected for detailed evaluation. Figure 6 presents the FTIR spectra of the polymer matrix at these glutaraldehyde (GA) concentrations, providing valuable insights into the chemical changes induced by increasing crosslinker content. The spectra focus on the O–H stretching vibrations (3000–3600 cm<sup>−1</sup>) and C–O–C stretching vibrations (1050–1200 cm<sup>−1</sup>), which are commonly reported as indicators of acetal linkage formation<sup>26</sup>. For comparison, the spectrum of the polymer matrix without glutaraldehyde is also included, serving as a baseline.

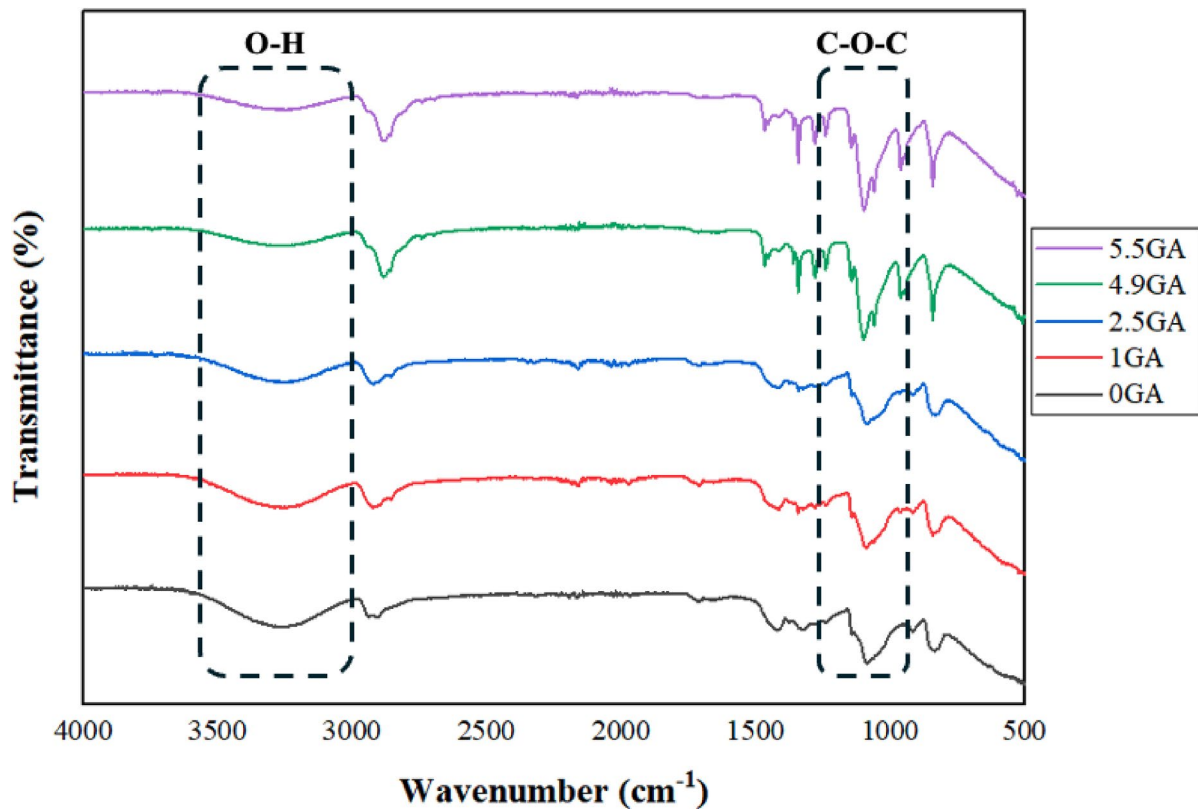


**Fig. 6.** FTIR spectrum of PVA-PEG-BTB film with glutaraldehyde concentrations of 0%, 1%, 2.5%, 4.9%, and 5.5%.

The O-H stretching band significantly diminishes as GA concentration increases, reflecting the gradual depletion of hydroxyl groups involved in the crosslinking reaction. This reduction in O-H stretching is associated with the formation of acetal linkages connecting glutaraldehyde to the hydroxyl groups within the polymer matrix<sup>26</sup>. The decrease in O-H is particularly evident at higher GA concentrations, as also shown in Supplementary Figure S2, which includes spectra for 7 wt% and 10 wt% GA.

Simultaneously, the C-O-C stretching band becomes more pronounced at higher GA concentrations (4.9 wt% and above), indicating the formation of acetal linkages. The presence of the C-O-C band remains evident even at higher GA concentrations, as shown in Supplementary Figure S2, further supporting the extensive formation of acetal linkages in the polymer network.

The SEM images of the polymeric films at varying glutaraldehyde concentrations (1, 2.5, 4.9, and 5.5 wt/wt%) are presented in Fig. 7. At 1 wt/wt% glutaraldehyde (Fig. 7a), the polymer exhibits a loosely organized structure characterized by larger and irregular voids. With an increase in glutaraldehyde concentration to 2.5 wt/wt% (Fig. 7b), the polymer network becomes denser and more uniform. At higher concentrations (4.9 and 5.5 wt/wt%), the micrographs reveal a progressively compact structure. At 5.5 wt/wt% glutaraldehyde (Fig. 7d), the polymer network appears excessively compact and rigid compared to the 4.9 wt/wt% sample (Fig. 7c).

#### Statistical evaluation using analysis of variance (ANOVA)

The single-factor ANOVA analysis, as shown in Table 4, demonstrates a statistically significant difference between glutaraldehyde concentration and swelling ratio, as indicated by the *p*-value of 2.1E- 161. This value is effectively zero and well below the established significance level ( $\alpha = 0.05$ ). This extremely low *p*-value highlights the robustness of the relationship between glutaraldehyde concentration and swelling behavior. It aligns with the fundamental understanding of glutaraldehyde's role as a crosslinking agent. By altering the polymer matrix's network structure, glutaraldehyde concentration significantly influences water absorption and swelling properties. This result provides compelling evidence that glutaraldehyde concentration is a critical determinant of the swelling behavior of the polymer.

#### Discussion

The results demonstrate that glutaraldehyde concentration plays a critical role in the swelling behavior and structural integrity of PVA-PEG-BTB films. The observed swelling peak at 4.9 wt% GA suggests an optimal crosslinking density that enhances hydrophilicity while maintaining polymer flexibility. Beyond this concentration, excessive crosslinking restricts water diffusion, leading to a decline in swelling capacity. The balance between swelling behavior and gel integrity is evident in the comparison of swelling ratio and gel fraction. At 4.9 wt% GA, the polymer network achieves maximum swelling due to improved hydrophilicity

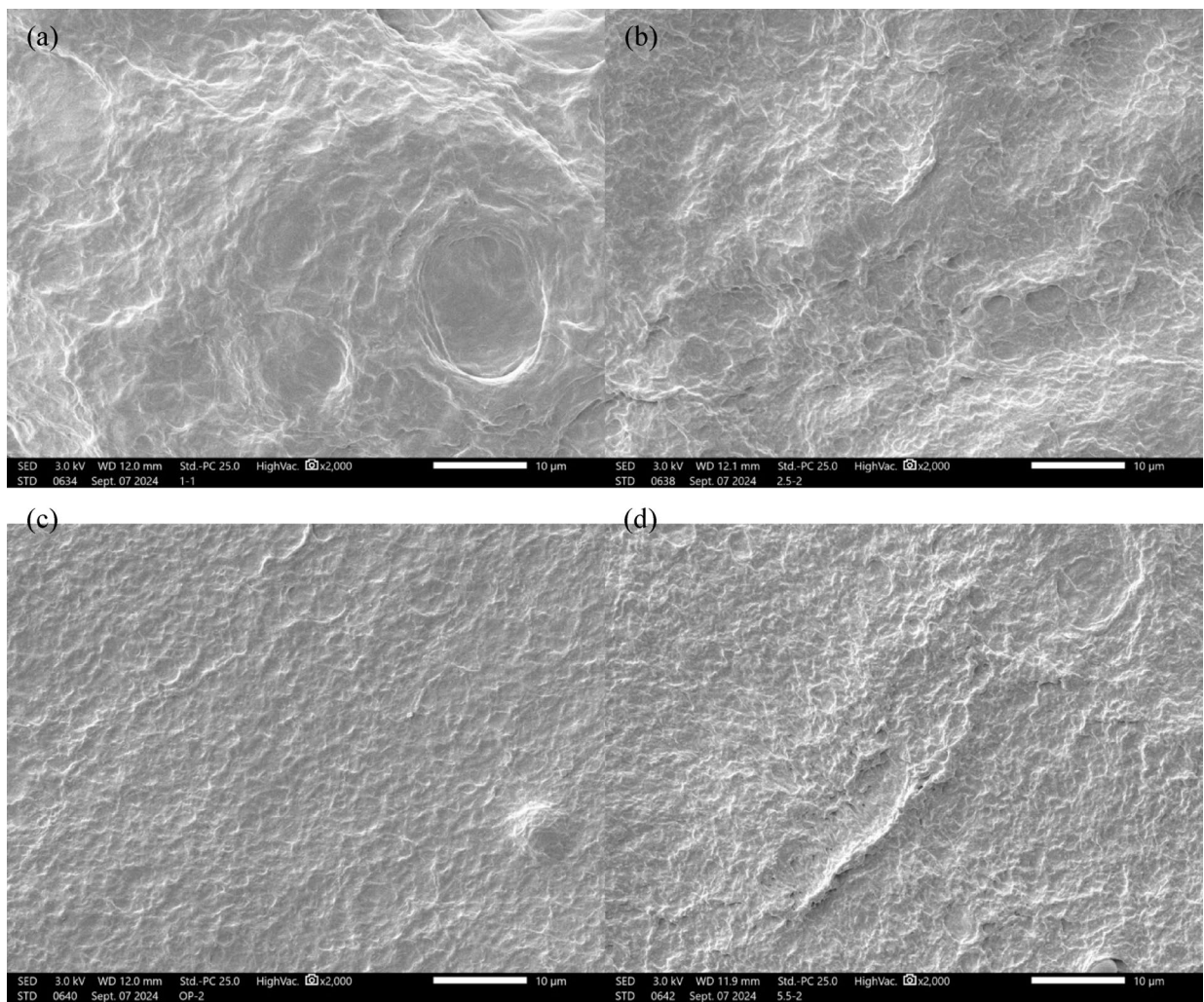


**Fig. 7.** SEM image of PVA-PEG-BTB film with glutaraldehyde concentration of (a) 1wt/wt%, (b) 2.5 wt/wt%, (c) 4.9 wt/wt%, and (d) 5.5 wt/wt%.

Source	Sum of squares	Degree of freedom	Mean square	F	p-value
Between groups	61588817.7	1	61588817.7	4180.4	2.1e <sup>-161</sup>
Within groups	3801024.6	258	14732.7		
Total	65389842.3	259			

**Table 4.** ANOVA results.

while maintaining moderate gel stability. However, higher GA concentrations lead to a more rigid structure, reducing flexibility, decreasing hydrophilic site availability, and limiting free volume. This trend is further supported by FTIR analysis, which reveals that increased GA concentrations deplete hydroxyl groups, thereby reducing hydrophilicity while promoting acetal linkage formation that rigidifies the polymer matrix. SEM images confirm these findings, illustrating a densely packed, rigid structure at 5.5 wt% GA, indicative of over-crosslinking. The successful implementation of hybrid genetic metaheuristic algorithms in optimizing GA concentration highlights the effectiveness of AI-driven approaches in material optimization. Among the three tested algorithms, HG-HLOA exhibited superior convergence and accuracy, consistently identifying 4.9251 wt% GA as the optimal concentration. The close agreement (0.65% deviation) between experimental and predicted swelling ratios underscores the reliability of the proposed fitness function. Additionally, a comparative analysis with previous studies demonstrates the advantages of hybrid genetic optimization over RSM-based approaches, particularly in reducing prediction error. The 0.65% deviation observed in this study is significantly lower than the deviations reported in prior RSM studies (up to 8.84% for swelling ratio prediction), highlighting the robustness and precision of the hybrid genetic framework. Despite these advancements, this study is limited to single-variable optimization, which may overlook potential interactions between polymeric components. Future

research should explore multi-variable optimization, incorporating factors such as plasticizer concentration, dye loading, and additional crosslinking agents to further refine hydrogel performance. Expanding this approach could lead to the development of highly tunable polymeric films, enhancing their applicability in biomedical and wound care applications.

## Conclusion

This study successfully optimized the swelling behavior of PVA-PEG-BTB films by systematically analyzing the effects of glutaraldehyde concentration and applying hybrid genetic metaheuristic algorithms for model-driven optimization. The optimal glutaraldehyde concentration was determined as 4.9251 wt%, yielding a predicted maximum swelling ratio of 1217.7311%. Experimental validation produced an average swelling ratio of 1225.7123%, showing a minimal deviation of only 0.65% from the predicted value, thereby confirming the model's reliability. Statistical analysis using ANOVA revealed a highly significant relationship between glutaraldehyde concentration and swelling behavior, with a p-value of 2.1E- 161. Beyond the optimal concentration, a decline in swelling capacity was observed, likely due to excessive crosslinking and the formation of acetal linkages, which reduces free volume and limits water uptake. This trend was further supported by FTIR and SEM analyses, which revealed structural changes consistent with increasing crosslinking density.

The application of HG-HLOA as an optimization tool proved highly effective, achieving superior convergence and prediction accuracy with minimal deviation between experimental and model-predicted values. The comparison with RSM-based studies highlights the advantages of hybrid genetic algorithms in reducing prediction error and improving optimization efficiency.

These results provide valuable insights into tunable polymer network design, particularly for wound care applications where swelling properties are critical. The optimized GA concentration enhances water absorption while maintaining structural integrity, offering a potential pathway for smart hydrogel development. Future studies could further investigate the dynamic swelling behavior of the hydrogel under different physiological conditions, including variations in temperature, ionic strength, and simulated wound exudates. This would provide deeper insights into its real-world performance and adaptability in clinical applications. Additionally, exploring multi-objective optimization, long-term stability, and biocompatibility testing can further enhance the formulation's effectiveness. The optimization framework and insights gained in this study can also inform the design and improvement of other hydrogel systems for both biomedical and industrial applications.

## Methods

### Materials

Polyvinyl alcohol (PVA) with a viscosity of 50–60 mPa·s and a degree of hydrolysis of 97–99%, along with polyethylene glycol 6000, were procured from Xilong Scientific (China). Bromothymol blue was obtained from Sinopharm Chemical Reagent (China), while glutaraldehyde (50 wt% in H<sub>2</sub>O) was sourced from Sigma-Aldrich (USA).

### Synthesis of PVA-PEG-BTB film

The synthesis process for the PVA-PEG-BTB film was adapted from our previous study with minimal modifications<sup>27</sup>. A 10% (w/v) PVA solution was prepared by dissolving PVA in distilled water while maintaining the temperature between 70 °C and 90 °C. Simultaneously, an 8% (w/v) PEG solution was prepared. Once both solutions achieved homogeneity, they were combined, and 0.03% (w/v) BTB powder was added.

To initiate crosslinking, glutaraldehyde at varying concentrations (0.5–6 wt%) was incorporated into the mixture, which was then stirred for an additional 30 min. The resulting solution was poured into silicone molds and dried at 60 °C for 4 h using a Shel Lab 1600 convection oven.

### Data collection through swelling test

Following the protocol described above, a total of 12 solution variations were prepared, each with a different glutaraldehyde concentration. The concentrations ranged from 0.5 to 6%, with increments of 0.5%. For each solution, 10 PVA-PEG-BTB film samples were fabricated, resulting in a total of 120 samples.

The dried weight ( $W_d$ ) of each sample was recorded before immersion in 30 mL of distilled water. At 10-minute intervals, the swollen weight ( $W_s$ ) of each sample was measured after carefully removing excess water. This process was repeated for 90 min for each sample, and the swelling ratio was calculated using Eq. (2).

$$\text{Swelling ratio (\%)} = \frac{W_s - W_d}{W_d} \times 100 \quad (2)$$

The maximum swelling ratio for each sample was measured and documented, producing a dataset consisting of 120 entries.

### Optimization using hybrid genetic metaheuristic algorithms

This part consists of two main steps: (1) generating the fitness function from the raw dataset and (2) performing the optimization process using various metaheuristic algorithms. All steps in this section were executed using MATLAB software. The dataset, which includes glutaraldehyde (GA) concentration as the input variable and the maximum swelling ratio as the output variable, was processed using the genetic programming toolbox. The hyperparameters employed for generating the fitness function through genetic programming are detailed in Table 5.

The parameter values used in the genetic programming process were carefully selected to balance computational efficiency, solution accuracy, and model interpretability, guided by standard practices, prior

Hyperparameter	Value
Population size	100
Maximum generations	100
Tournament size	50
Elite fraction	0.1
Probability of pareto tournament	0.8
Maximum genes	15
Maximum tree depth	15
Crossover probability	0.84
Mutation probability	0.14

**Table 5.** Hyperparameters used in genetic programming.

literature, and iterative testing. The population size and maximum number of generations were chosen to ensure a diverse initial solution pool and sufficient evolutionary iterations for convergence without excessive computational costs. The tournament size and elite fraction were set to maintain diversity during selection while ensuring that the best-performing solutions were preserved across generations to guide optimization effectively.

Additionally, constraints on the number of genes and tree depth were applied to prevent overcomplexity in the evolved models, promoting interpretability and reducing the risk of overfitting. Crossover and mutation probabilities were adjusted to promote the effective combination of high-performing solutions while introducing diversity to investigate unexplored areas of the solution space and avoid early convergence. The selected parameters collectively reflect a systematic approach to optimizing the genetic programming process, ensuring robust performance while maintaining computational feasibility and practical applicability.

The optimization process utilized three distinct metaheuristic algorithms: the Hippopotamus Optimizer (HO), Walrus Optimization Algorithm (WOA), and Horned Lizard Optimization Algorithm (HLOA). The fitness function generated earlier was used to identify the optimal value of GA concentration for each algorithm. The convergence behavior of each algorithm was analyzed to identify the best-performing approach. Following this, a new set of PVA-PEG-BTB films was fabricated based on the optimized GA concentrations, and swelling tests were conducted to validate the optimization results. The pseudocode of the hybrid genetic metaheuristic algorithms utilized in this study is presented below.

<p><b>(a) Algorithm 1</b> Hybrid Genetic Hippopotamus Optimization Algorithm</p> <pre> 1: Initialize population of symbolic expressions 2: Define the maximum number of generations (MaxGen) and population size    (PopSize) 3: Define the fitness function for symbolic regression 4: Evaluate the fitness of each symbolic expression in the population 5: Identify the best symbolic expression (BestExpression) based on fitness 6: for generation = 1 to MaxGen do 7:   for each symbolic expression in the population do 8:     Apply genetic operations: 9:       - Crossover: Exchange subtrees between parent expressions 10:      - Mutation: Replace a random subtree with a newly generated subtree 11:      - Reproduction: Copy the best-performing individuals to the next genera-       tion 12:      Ensure the offspring adheres to constraints (e.g., tree depth) 13:   end for 14:   Evaluate the fitness of the new population 15:   Update BestExpression if a better solution is found 16:   if termination criteria are met (e.g., fitness threshold or MaxGen reached) then 17:     break 18:   end if 19: end for 20: Define the best symbolic expression (BestExpression) as the    ObjectiveFunction 21: Initialize population of hippos (solutions) randomly within the search space 22: Define the maximum number of iterations (MaxIter) 23: Evaluate the fitness of each hippo in the population using ObjectiveFunction 24: Identify the best solution (BestHippo) based on fitness 25: for iteration = 1 to MaxIter do 26:   for each hippo in the population do 27:     Phase 1: Positioning in the River or Pond (Exploration) 28:     Calculate the new position based on random movement toward water       sources 29:     Introduce diversity in the search space using stochastic components 30:     Phase 2: Defense Against Predators (Local Refinement) 31:     Adjust the position by interacting with nearby hippos 32:     Fine-tune the solution in promising regions of the search space 33:     Phase 3: Escaping from Predators (Global Search) 34:     Apply a large random movement to simulate escaping behavior 35:     Diversify the position to avoid local optima 36:     Enforce boundary constraints to keep solutions within the search space 37:     Evaluate the fitness of the updated position using ObjectiveFunction 38:   end for 39:   Update BestHippo if a better solution is found 40:   if termination criteria are met (e.g., fitness threshold or MaxIter reached) then 41:     break 42:   end if 43: end for 44: return BestHippo as the optimal solution </pre>	<p><b>(b) Algorithm 2</b> Hybrid Genetic Walrus Optimization Algorithm</p> <pre> 1: Initialize population of symbolic expressions 2: Define the maximum number of generations (MaxGen) and population size    (PopSize) 3: Define the fitness function for symbolic regression 4: Evaluate the fitness of each symbolic expression in the population 5: Identify the best symbolic expression (BestExpression) based on fitness 6: for generation = 1 to MaxGen do 7:   for each symbolic expression in the population do 8:     Apply genetic operations: 9:       - Crossover: Exchange subtrees between parent expressions 10:      - Mutation: Replace a random subtree with a newly generated subtree 11:      - Reproduction: Copy the best-performing individuals to the next genera-       tion 12:      Ensure the offspring adheres to constraints (e.g., tree depth) 13:   end for 14:   Evaluate the fitness of the new population 15:   Update BestExpression if a better solution is found 16:   if termination criteria are met (e.g., fitness threshold or MaxGen reached) then 17:     break 18:   end if 19: end for 20: Define the best symbolic expression (BestExpression) as the    ObjectiveFunction 21: Initialize population of walruses (solutions) randomly within the search space 22: Define the maximum number of iterations (MaxIter) 23: Evaluate the fitness of each walrus in the population using ObjectiveFunction 24: Identify the best solution (BestWalrus) based on fitness 25: for iteration = 1 to MaxIter do 26:   for each walrus in the population do 27:     Phase 1: Feeding Strategy (Exploration) 28:     Calculate the new position based on feeding behavior 29:     Introduce diversity in the search space by exploring nearby regions 30:     Phase 2: Migration (Local and Global Search) 31:     Adjust position to simulate migration toward favorable areas 32:     Balance between local refinement and global exploration during migra-       tion 33:     Phase 3: Escaping and Fighting Against Predators (Global Diversifi-       cation) 34:     Apply a random movement to simulate escaping from predators 35:     Introduce large, unpredictable changes to escape local optima and ex-       plore globally 36:     Enforce boundary constraints to keep solutions within the search space 37:     Evaluate the fitness of the updated position using ObjectiveFunction 38:   end for 39:   Update BestWalrus if a better solution is found 40:   if termination criteria are met (e.g., fitness threshold or MaxIter reached) then 41:     break 42:   end if 43: end for 44: return BestWalrus as the optimal solution </pre>
<p><b>(c) Algorithm 3</b> Hybrid Genetic Horned Lizard Optimization Algorithm</p> <pre> 1: Initialize population of symbolic expressions 2: Define MaxGen, PopSize, and the fitness function 3: Evaluate fitness and identify the best expression (BestExpression) 4: for generation = 1 to MaxGen do 5:   for each symbolic expression do 6:     Apply Genetic Operations: 7:       - Crossover: Swap subtrees 8:       - Mutation: Replace a random subtree 9:       - Reproduction: Copy top-performing solutions 10:   end for 11:   Update BestExpression if a better solution is found 12:   if termination criteria met (fitness threshold or MaxGen reached) then 13:     break 14:   end if 15: end for 16: Define BestExpression as the ObjectiveFunction for optimization 17: Initialize horned lizard population within the search space 18: Define MaxIter and evaluate fitness to find BestLizard 19: for iteration = 1 to MaxIter do 20:   for each lizard do 21:     if Crypsis then 22:       Strategy 1: Crypsis - Mimic surroundings 23:     else if Flee then 24:       Strategy 2: Move-to-Escape - Random movement 25:     else 26:       Strategy 3: Bloodstream Shoot - Unpredictable motion 27:     end if 28:   end for 29:   Replace worst agents (Strategy 4: Skin Darkening/Lightening) 30:   if Low A-Melanophore Rate? then 31:     Strategy 5: Replace Search Agents 32:   end if 33:   Update BestLizard if a better solution is found 34:   if termination criteria met (fitness threshold or MaxIter reached) then 35:     break 36:   end if 37: end for 38: return BestLizard as the optimal solution </pre>	

**Algorithm 1.** Pseudocode of (a) hybrid genetic hippopotamus optimization algorithm, (b) hybrid genetic walrus optimization algorithm, (c) hybrid genetic horned lizard optimization algorithm.

## PVA-PEG-BTB film characterization and analysis

### Gel fraction test

The initial weight ( $W_i$ ) of the dried samples containing glutaraldehyde was documented before immersion in a Petri dish filled with distilled water. The samples were left for 24 h to reach equilibrium. Afterward, excess water was carefully removed, and the samples were oven-dried at 60 °C for 4 h. The final weight ( $W_f$ ) of the undissolved content was then measured. The gel fraction, defined as the ratio of the insoluble portion of the polymeric network to the total initial weight of the sample, represents the degree of crosslinking within the polymer matrix, and it was calculated using Eq. (3).

$$\text{Gel fraction (\%)} = \frac{W_f}{W_i} \times 100 \quad (3)$$

### Spectroscopic and morphological analysis

Fourier-transform infrared (FTIR) analysis of the dried samples was performed using an Agilent Cary 630 FTIR Spectrometer. Dried samples were sputter-coated with a thin gold layer to improve conductivity for scanning electron microscopy (SEM) analysis. Imaging was conducted using a JEOL JSM IT500HR/LA Schottky Field Emission SEM, operating in High Vacuum Mode at 30 kV with a resolution of 1.5 nm. Each image was captured at a magnification of 2,000x.

### Statistical analysis

A statistical analysis was conducted to assess the significance of differences between the experimental groups. A one-way analysis of variance (ANOVA) was conducted to examine the impact of independent variables on the response parameters. The analysis was conducted to test the null hypothesis, stating that no significant differences existed between the group means, with a 95% confidence level ( $p < 0.05$ ). The ANOVA was executed using Microsoft Excel.

## Data availability

The datasets used and/or analyzed during the current study are available from the corresponding author upon request.

Received: 3 February 2025; Accepted: 1 April 2025

Published online: 12 April 2025

## References

- Alavarce, A. C. et al. Crosslinkers for polysaccharides and proteins: Synthesis conditions, mechanisms, and crosslinking efficiency, a review. *International Journal of Biological Macromolecules* vol. 202 558–596 Preprint at (2022). <https://doi.org/10.1016/j.ijbiomac.2022.01.029>
- Grabska-Zielinska, S. Cross-Linking Agents in Three-Component Materials Dedicated to Biomedical Applications: A Review. *Polymers* vol. 16 Preprint at (2024). <https://doi.org/10.3390/polym16182679>
- Metze, F. K. et al. Soft Mechanochemistry in Polymer Materials. *Langmuir* vol. 39 3546–3557 Preprint at (2023). <https://doi.org/10.1021/acs.langmuir.2c02801>
- Massarelli, E. et al. Polyvinyl alcohol/chitosan wound dressings loaded with antisepsics. *Int. J. Pharm.* **593**, (2021).
- Tamer, T. M. et al. Hemostatic and antibacterial PVA/Kaolin composite sponges loaded with penicillin-streptomycin for wound dressing applications. *Sci. Rep.* **11**, (2021).
- Bustamante-Torres, M. et al. Hydrogels classification according to the physical or chemical interactions and as Stimuli-Sensitive materials. *Gels* **7**, 182 (2021).
- Hoti, G. et al. Effect of the cross-linking density on the swelling and rheological behavior of ester-bridged  $\beta$ -cyclodextrin nanosponges. *Materials* **14**, 1–20 (2021).
- Kumari, M. & Gupta, S. K. Response surface methodological (RSM) approach for optimizing the removal of trihalomethanes (THMs) and its precursor's by surfactant modified magnetic nanoadsorbents (sMNP) - An endeavor to diminish probable cancer risk. *Sci. Rep.* **9**, (2019).
- Wang, J. et al. Optimization of reaction conditions by RSM and structure characterization of sulfated locust bean gum. *Carbohydr. Polym.* **114**, 375–383 (2014).
- Elganidi, I., Elarbe, B., Ridzuan, N. & Abdullah, N. Optimisation of reaction parameters for a novel polymeric additives as flow improvers of crude oil using response surface methodology. *J. Pet. Explor. Prod. Technol.* **12**, 437–449 (2022).
- Martin, T. B. & Audus, D. J. Emerging trends in machine learning: A polymer perspective. *ACS Polym. Au.* **3**, 239–258 (2023).
- Kim, D., Concepcion, R. S., Espiritu, G. A. M., Rey, J. & Vicerra, R. R. P. J. R. H. Optimized Fuzzy Logic and Adaptive Neuro-Fuzzy Inference Systems for Wound Healing Time Prediction Among the Diabetic Patients. in 2023 8th International Conference on Business and Industrial Research, ICBIR 2023 - Proceedings 536–542 Institute of Electrical and Electronics Engineers Inc., (2023). <https://doi.org/10.1109/ICBIR57571.2023.10147571>
- Nemati, M., Zandi, Y. & Agdas, A. S. Application of a novel metaheuristic algorithm inspired by stadium spectators in global optimization problems. *Sci. Rep.* **14**, (2024).
- Agrawal, P., Abutarboush, H. F., Ganesh, T. & Mohamed, A. W. Metaheuristic algorithms on feature selection: A survey of one decade of research (2009–2019). *IEEE Access* **9**, 26766–26791 (2021).
- Xu, M., Cao, L., Lu, D., Hu, Z. & Yue, Y. Application of Swarm Intelligence Optimization Algorithms in Image Processing: A Comprehensive Review of Analysis, Synthesis, and Optimization. *Biomimetics* vol. 8 Preprint at (2023). <https://doi.org/10.3390/biomimetics8020235>
- Hamadneh, T. et al. Fossa optimization algorithm: A new Bio-Inspired metaheuristic algorithm for engineering applications. *Int. J. Intell. Eng. Syst.* **17**, 1038–1047 (2024).
- Hamadneh, T. et al. Orangutan optimization algorithm: an innovative Bio-Inspired metaheuristic approach for solving engineering optimization problems. *Int. J. Intell. Eng. Syst.* **18**, 81–92 (2025).
- Hamadneh, T. et al. Spider-Tailed horned Viper optimization: an effective Bio-Inspired metaheuristic algorithm for solving engineering applications. *Int. J. Intell. Eng. Syst.* **18**, 25–35 (2025).
- Amiri, M. H., Hashjin, M., Montazeri, N., Mirjalili, M. & Khodadadi, N. S. Hippopotamus optimization algorithm: a novel nature-inspired optimization algorithm. *Sci. Rep.* **14**, (2024).

20. Trojovský, P. & Dehghani, M. A new bio-inspired metaheuristic algorithm for solving optimization problems based on walruses behavior. *Sci. Rep.* **13**, (2023).
21. Peraza-Vázquez, H., Peña-Delgado, A., Merino-Treviño, M. & Morales-Cepeda, A. B. & Sinha, N. A novel metaheuristic inspired by horned Lizard defense tactics. *Artif. Intell. Rev.* **57**, (2024).
22. Kaliampakou, C., Lagopati, N., Pavlatou, E. A. & Charitidis, C. A. Alginates–Gelatin Hydrogel Scaffolds; An Optimization of Post-Printing Treatment for Enhanced Degradation and Swelling Behavior. *Gels* **9**, (2023).
23. Said, N. S. & Sarbon, N. M. Response surface methodology (RSM) of chicken skin gelatin based composite films with rice starch and Curcumin incorporation. *Polym. Test.* **81**, (2020).
24. Kim, K. J., Lee, S. B. & Han, N. W. Effects of the degree of crosslinking on properties of Poly(Vinyl Alcohol) Membranes. *Polym. J.* **25** (1993).
25. Mohammad Mahdi Dadfar, S., Kavoosi, G., Mohammad, A. & Dadfar, S. Investigation of mechanical properties, antibacterial features, and water vapor permeability of Polyvinyl alcohol thin films reinforced by glutaraldehyde and multiwalled carbon nanotube. *Polym. Compos.* **35**, 1736–1743 (2014).
26. Blanco-Covián, L., Campello-García, J. R., Blanco-López, M. C. & Miranda-Martínez, M. Synthesis, characterization and evaluation of the antibiofouling potential of some metal and metal oxide nanoparticles. *Appl. Sci. (Switzerland)* **10**, (2020).
27. Kim, D., Concepcion, R. S., Sta. Agueda, J. R. H. & Mondragon, J. M. S. Optimizing recurrent neural Network-Based pH prediction system of halochromic film for chronic wound monitoring. *IEEE Access* **12**, 88756–88766 (2024).

## Acknowledgements

The authors extend their gratitude to the Biomaterials and Tissue Engineering Laboratories (BiMaTEL) under the Center of Engineering and Sustainable Development Research, De La Salle University, for their invaluable support and resources. This research was funded by the Department of Science and Technology – Philippine Council for Health Research and Development (DOST-PCHRD) through the Smart Multifunctional and Indigenous Dressings Sterilized Using Electron Beam as Novel Wound Repair Matrices (SMIDERM) Project.

## Author contributions

D.K. conceptualized the research, performed the experiments, and led the optimization process. I.N.M.D.C. contributed to writing the manuscript, and R.S.C. provided supervision for data interpretation and guided the optimization strategies. T.M.S.M. supervised the experimental work, while both T.M.S.M. J.R.H.S., and R.K.B.B. offered valuable insights into the interpretation of the material properties and results. All authors contributed to the manuscript revision and provided critical feedback to enhance the final version.

## Funding

This study was funded by Philippine Council for Health Research and Development.

## Declarations

### Competing interests

The authors declare no competing interests.

### Additional information

**Supplementary Information** The online version contains supplementary material available at <https://doi.org/10.1038/s41598-025-96953-0>.

**Correspondence** and requests for materials should be addressed to D.K.

**Reprints and permissions information** is available at [www.nature.com/reprints](http://www.nature.com/reprints).

**Publisher's note** Springer Nature remains neutral with regard to jurisdictional claims in published maps and institutional affiliations.

**Open Access** This article is licensed under a Creative Commons Attribution-NonCommercial-NoDerivatives 4.0 International License, which permits any non-commercial use, sharing, distribution and reproduction in any medium or format, as long as you give appropriate credit to the original author(s) and the source, provide a link to the Creative Commons licence, and indicate if you modified the licensed material. You do not have permission under this licence to share adapted material derived from this article or parts of it. The images or other third party material in this article are included in the article's Creative Commons licence, unless indicated otherwise in a credit line to the material. If material is not included in the article's Creative Commons licence and your intended use is not permitted by statutory regulation or exceeds the permitted use, you will need to obtain permission directly from the copyright holder. To view a copy of this licence, visit <http://creativecommons.org/licenses/by-nc-nd/4.0/>.

© The Author(s) 2025